Earth and Planetary Science Letters 457 (2017) 292–301

Contents lists available at ScienceDirect

Earth and Planetary Science Letters

www.elsevier.com/locate/epsl

Vertical tectonics at an active continental margin

N. Houlié [a,b,*], T.A. Stern [c]

[a] Institute of Geophysics (SEG), Earth Sciences Department (ERDW), ETH-Zurich, Zurich, Switzerland
[b] Mathematical Physical Geodesy (MPG), Institut für Geodäsie und Photogrammetrie, ETH-Zurich, Zurich, Switzerland
[c] Victoria University, Wellington, New Zealand

ARTICLE INFO

Article history:
Received 23 June 2016
Received in revised form 11 October 2016
Accepted 13 October 2016
Available online 2 November 2016
Editor: P. Shearer

Keywords:
subduction
plate boundary
uplift
GPS
New Zealand
seismology

ABSTRACT

Direct observations of vertical movements of the earth's surface are now possible with space-based GPS networks, and have applications to resources, hazards and tectonics. Here we present data on vertical movements of the Earth's surface in New Zealand, computed from the processing of GPS data collected between 2000 and 2015 by 189 permanent GPS stations. We map the geographical variation in vertical rates and show how these variations are explicable within a tectonic framework of subduction, volcanic activity and slow slip earthquakes. Subsidence of >3 mm/yr is observed along southeastern North Island and is interpreted to be due to the locked segment of the Hikurangi subduction zone. Uplift of 1–3 mm/yr further north along the margin of the eastern North Island is interpreted as being due to the plate interface being unlocked and underplating of sediment on the subduction thrust. The Volcanic Plateau of the central North Island is being uplifted at about 1 mm/yr, which can be explained by basaltic melts being injected in the active mantle-wedge at a rate of ~6 mm/yr. Within the Central Volcanic Region there is a 250 km^2 area that subsided between 2005 and 2012 at a rate of up to 14 mm/yr. Time series from the stations located within and near the zone of subsidence show a strong link between subsidence, adjacent uplift and local earthquake swarms.

1. Introduction

Most tectonic studies based on GPS have focused on the horizontal components of velocity (Thatcher, 2003), as these are more accurately determined than the vertical rate. The reason for this is that tropospheric changes and satellite constellation geometry issues compromise the estimates of vertical velocities more than that of the horizontal ones (Houlié et al., 2016). Arrays of continuous GPS instruments (C-GPS) that were installed more than a decade ago are now providing surface vertical rates that could be compared to long-term estimates (Beavan et al., 2010).

Vertical velocities are important because they provide different constraints, compared to horizontal velocities, on processes in the Earth such as dynamics of the upper mantle (Gurnis et al., 1998; Molnar, 2015), glacial isostatic adjustment (Bradley et al., 2009; Sella et al., 2007; Teferle et al., 2009), erosion rates (Cox et al., 2012; Herman et al., 2010; Nibourel et al., 2015), stability of mountains belts (Ching et al., 2011; Hammond et al., 2012; Houlié et al., submitted for publication; Koons, 1990; Liang et al., 2013; Serpelloni et al., 2013), spatial variations in the coupling of a subduction thrust (Kaneko et al., 2010; Savage, 1983) or crustal thinning (Steckler, 1985). There are also evolving practical applications for C-GPS data to monitoring water tables (Amos et al., 2014) and detecting locked faults (Howell et al., 2016; Lamb and Smith, 2013). Plate boundary settings are particularly favorable locations for these studies because the rates of vertical movement tend to be relatively large (>2 mm/yr).

Both GPS and geodetic solutions of vertical and horizontal velocities within plate boundary zones result from short- (year to decades) and long-term (million years) processes. For example, in New-Zealand, vertical rates have been used to constrain shortening rates across the Alpine fault (Beavan et al., 2010, 2004), and to provide insight to both the level of incompressibility of the lithosphere (Houlié and Stern, 2012), and the extent of the locked segments of the subducted Pacific plate slab along the Hikurangi margin (Lamb and Smith, 2013). In this study we present the first surface uplift map for New Zealand based on GPS and discuss its implications for tectonic processes.

2. Data

We processed GPS data collected by the GEONET-NZ network (Fig. 1) for the period spanning from January 2000 to March

* Corresponding author.
E-mail address: nhoulie@ethz.ch (N. Houlié).

http://dx.doi.org/10.1016/j.epsl.2016.10.018
0012-821X/

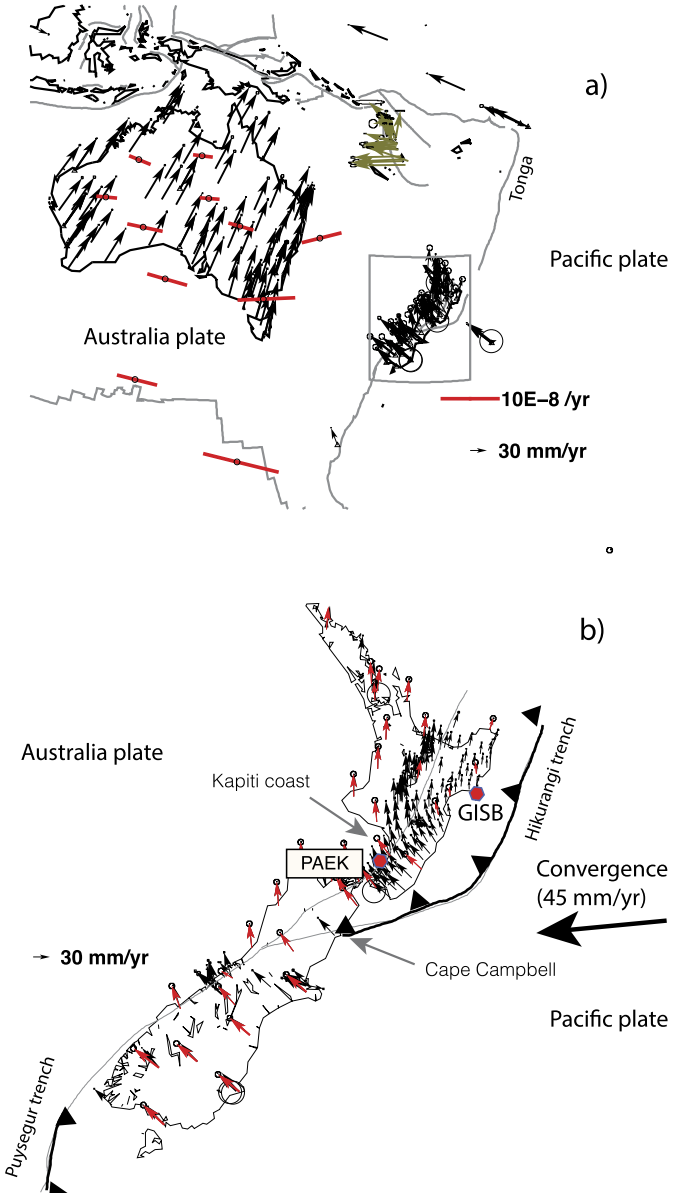

Fig. 1. a) Surface motions in the surroundings of East Australia plate and New Zealand. b) Velocities of New Zealand GEONET cGPS stations (www.geonet.org.nz) obtained by Houlié and Stern (2012) are compared with those presented in this study (black). All velocities are shown in the ITRF08 (Altamimi et al., 2012). Green and red vectors are from Bergeot et al. (2009) and Houlié and Stern (2012), respectively. (For interpretation of the references to color in this figure legend, the reader is referred to the web version of this article.)

2015 using GAMIT (King and Bock, 2012). As the complete dataset was too big to be processed as one, we divided it into five sub-networks; each of them including the same reference sites (AUCK, CHAT, CHTI, GUAM, OUS2 and WGTN, see Fig. A1 of Supplementary materials) for which we know positions and velocities with high accuracy from the ITRF2008 (Altamimi et al., 2012). Using this backbone network, daily solutions were combined using GLOBK/GLORG (Herring, 2003) by minimizing the shift between the ITRF2008 solutions (Altamimi et al., 2012) and ours. All rates were computed using a linear regression assuming uncertainties of east, north and vertical components were equal to 2.0, 2.0 and 5.0 mm, respectively.

We took into account the disruption of trends generated by large seismic events. During the last decade, five major seismic events have occurred in the South Island of New Zealand in this period: Dusky Sound (Mw 7.8, 2009/07/15), Canterbury (Mw 7.1, 2010/09/04), Christchurch (Mw 6.3, 2011/02/22), Cook Strait (Mw 6.3, 2012/07/03) and Seddon (Mw = 6.5, 2013/07/21). These seismic events induced sharp discontinuities (coseismic) and smoother non-linear (post-seismic) motions of the closest sites. For those that have been affected, we introduce offsets in the time-series at the times of the earthquakes to minimize the impact of the co- and post-seismic deformation on interseismic rates. We did not remove data of the time-series. Another perturbation effect on the vertical uplift field is the occurrence, along the east of North Island, of slow slip events associated with the subducted Pacific plate (Delahaye et al., 2009; Wallace and Beavan, 2006, 2010). These events typically occur over periods of months to 5 yr and do not necessarily produce consistent patterns across the network, suggesting that regional filtering (Wdowinski et al., 1997) cannot be applied here without changing the overall pattern of the surface deformation. For these sites, rates ($\vec{v}$) should be described as "apparent" and decomposed as follows:

$$\vec{v} = \vec{V}_{int.} + \sum_{n=1}^{i} \frac{\vec{d}_{slow}}{\partial t}$$

where ∂t is the duration of each slow slip event and $\vec{d}_{slow}$ is the amount of vertical movement during a slow slip event. As $\vec{V}_{int.}$ and $\sum_{n=1}^{i}(\vec{d}_{slow})$ are of opposite signs they have opposite effects regarding the consequences of the global sea level rise occurring in the area. In this first study of cGPS for vertical uplift rates in New Zealand we have not tried to isolate the effect of slow slip as the cGPS time-series are still too short and corrections would require subjective judgments. Instead we note that, in the area where slow-slip events have occurred in the past 15 yr, computed rates are not truly representative of the interseismic deformation, but are only short-term apparent rates (Fig. 2). The equality between long-term inter-seismic rates and apparent ones depend on a complex function of both the number of slow slip events, and of their amplitudes. At the end of the process, horizontal velocities were available for 189 sites.

3. Results

3.1. Uncertainties

For 161 sites located in New Zealand, vertical rates were constrained with a formal accuracy of less than 2.0 mm/yr (Fig. 3). The vertical rate uncertainties depend on the number of operational days for each site in the network (Fig. 3). For 53 sites that are the oldest, with records >6 yr, an accuracy of <1 mm/yr was reached. In order to assess the quality of the GPS vertical rates, uncertainties reached after the combination of each sub-networks are plotted against the number of processed days for each station (Fig. 3c). Two parallel trends are visible in the station uncertainties pool: the stations with the lowest vertical uncertainties being those of the "LINZ" backbone array (www.geonet.org.nz). For those, uncertainty drops to less than 1 mm/yr after about 2000 days (~6 yr). Monuments quality, troposphere conditions and ground transients visible at the local scale are likely to be the main causes to explain why we observe two groups within the uncertainties data cloud.

3.2. The choice of level of reference for the vertical rates

In New Zealand, horizontal velocities are often referenced to a stable Australia plate although small strain rates ($<4.0 \times 10^{-8}$/yr) between Australia, Samoa and New Zealand can be inferred from regional GPS data analysis (Fig. 1). Choosing a reference for vertical rates is however less trivial. Geological estimates of uplift are

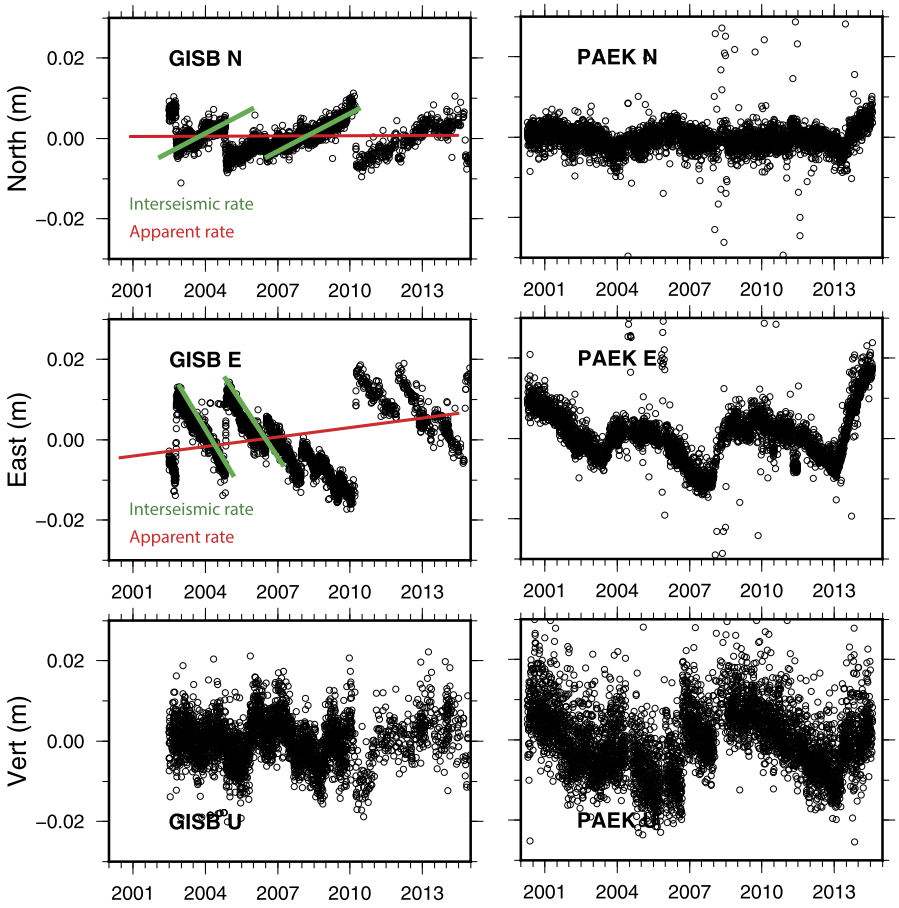

Fig. 2. Example of time-series of cGPS located near slow-slip event areas, after removal of linear trends (i.e. plate motion). Note that slow slip events make the determination of the interseismic rates more challenging than in other areas. After the removal of the long-period trend (red lines), because of the presence of discontinuities in the time-series, interseismic motion residuals are still visible (green lines). Interseismic rates are therefore not well described in the case of a large number of slow slip events (SSE) occurrences. (For interpretation of the references to color in this figure legend, the reader is referred to the web version of this article.)

generally referenced to sea level (e.g. terrace uplifts) or to a depth isotherm (i.e. fission track dating), but these are on a time scale different from cGPS. Uncertainty in the absolute vertical rate for a regional array can be of the order of 2 mm/yr (Teferle et al., 2009), yet relative uncertainties between stations of an array can still be <1 mm/yr.

In order to find an optimal base-line setting for the New Zealand array we consider geological constraints in order to place vertical GPS rates in an absolute framework that is effectively with respect to the center of the Earth. We adjust the GPS vertical rates on the long-term term motions in the region of Northland Peninsula near and north of Auckland (Fig. 4) where coastline motions with respect to the sea level are known to be close to zero (Beavan and Litchfield, 2012; Pillans, 1986, 1990) and this area is viewed as geologically and seismically stable compared to other parts of New Zealand (Eiby, 1958; Issac, 1996; Reyners, 1989). There are seven stations north of 37.5°S (KTAI, WHNG, WARK, AUCK, AUKT, CORM, HIKB; see supplementary material) for which the mean and standard deviation in velocities are -2.0 and 0.3 mm/yr respectively. The adjustment is therefore $+2.0$ mm/yr and is applied to the whole vertical rate dataset (Table 1, Fig. 3 and onwards).

3.3. General pattern

After the regional adjustment of $+2.0$ mm/yr the mean value of vertical velocity for the 161 Geonet stations is -0.4 ± 3.6 mm/yr (Fig. 3 and Table 1). Only two areas are subsiding: the east coast of the North Island near the locked segment of the subducted slab

Table 1
Average vertical rates, scattering and averaged formal errors for groups of sites identified in the main text. Hikurangi refers to stations within eastern North Island. Rates presented in this table were corrected of a 2.0 mm/yr bias (see main text for detailed explanations). A table of vertical rates and uncertainties for all cGPS stations are available in the Supplementary Materials. "Non-NZ" stations are permanent sites located outside New Zealand.

Uplift (mm/yr)	STDEV (mm/yr)	Unc. (mm/yr)	N sites	Group of sites excluded
0.1	2.9	1.2	149	Rotorua and non-NZ
0.5	3.1	1.2	119	Rotorua, non-NZ and Hikurangi
−1.6	1.1	1.1	32	All but Hikurangi
−8.6	4.5	1.3	9	All but Rotorua
−0.4	3.6	1.2	157	Non-NZ

(Figs. 3 and 4) and the region of volcanic subsidence close to Rotorua (Figs. 5a and 6), where horizontal contraction is predicted by Dimitrova et al. (2016). Elsewhere GPS uplift rates (Figs. 3 and 4) are in agreement with long-term estimates (Ota et al., 1996; Pillans, 1986). But rather than the absolute level of vertical motion for a specific station, what is important is the broad geographical consistency of uplift rates (Figs. 3, 4 and 5), that indicate the data are not merely random scatter but represent true tectonic processes at play on a regional (50–100 km) scale.

There are obvious exceptions to the regional pattern. Some stations (e.g. GISB, Figs. 2 and 3) illustrate that the time-scale needed for some stations to isolate transient motions requires to be longer than that available. Indeed, as shown by Beavan and Litchfield (2012), interseismic rates are difficult to capture at sites located

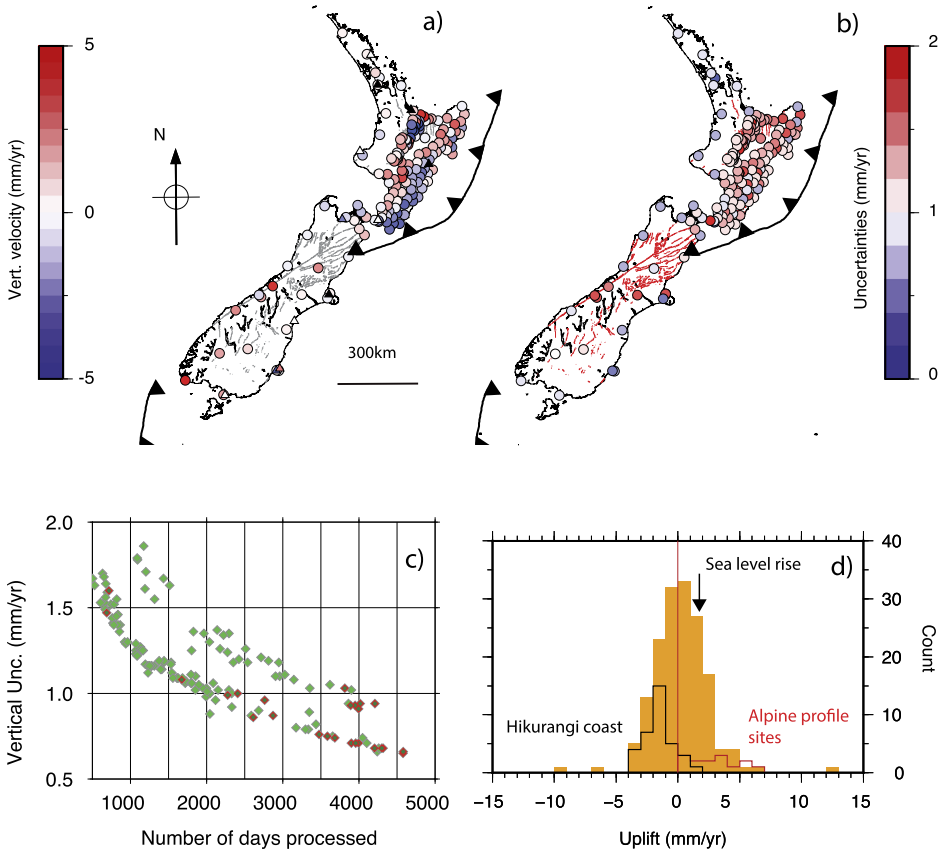

Fig. 3. Uplift rates (a) and associated uncertainties (b) for New Zealand adjusted as described in the text. (c) Uncertainties for cGPS stations plotted against number of days processed (green diamonds, in days). In supplementary materials, same plots are available for each subnetwork. Deep green diamonds are stations of the "LINZ" back bone array. (d) Distribution of uplift rates showing the approximate normal distribution with a mean of −0.4 mm/yr (standard deviation of 3.6 mm/yr, average uncertainty = 1.2 mm/yr). If the Rotorua stations are excluded, the mean is 0.1 mm/yr, std deviation = 2.9 mm/yr and the average uncertainty = 1.2 mm/yr. Rates for other station groups are presented in Table 1. We group as "Hikurangi" the sites located in eastern North Island along the Pacific coast. There is a spatial coincidence of the subsidence in this area with the area for which the subduction is thought to be locked. All rates are presented in the supplementary materials. For reference, campaign vertical rates constrained across Alpine fault by Beavan et al. (2010) are shown in red. Faults lines are from the GNS fault data base (https://data.gns.cri.nz/af/) (GNS New Zealand, 2015).

in the near field of slow-slip events. In the next 5–10 yr (depending on the number of SSEs in the future) we expect these stations to have enough data to discriminate interseismic and slow-slip periods, enabling us to constraint better inter-seismic rates (Fig. 2).

3.4. Local features

3.4.1. South Island

In the South Island, persistent uplift results from the continent-continent collision (Figs. 2 and 6), and is associated with crustal thickening (Scherwath et al., 2003). In particular, the strong uplift of 6–8 mm/yr is seen in central South Island and is co-located with both the convergence between Australia and New Zealand and the rise of the Southern Alps (Beavan et al., 2010). A large portion of the vertical velocity field detected here is likely to be the result of the crustal thickening linked to regional transpression (Lamb et al., 2015; Tikoff and Teyssier, 1994). Away from the Alpine fault, uplift rates are limited to 1–2 mm/yr like shown by Houlié and Stern (2012) with less data available. High vertical rates are nonetheless visible close to the Dusky Sound events where postseismic deformation of the event of 2009 is still ongoing.

3.4.2. North Island

In the North Island, diverse patterns of both uplift and subsidence are visible (Figs. 4 and 5.a and b). Along the northern section of eastern North Island there is uplift along the margin where the plate interface is freely slipping, yet where the plate interface appears to be locked (Walcott, 1984) at the southern end of the eastern North Island (Wellington City end) there is subsidence (Fig. 5b). Subsidence of southeastern North Island is consistent with the elastic dislocation model of Savage (1983). We assume half of the convergence rate is converted into shortening (22 mm/yr) with various values of downdip slip width s. Vertical rates along Profile 1 (Fig. 7a) are consistent with the interseismic deformation model whereas velocity profiles 3, 4 and 5 are not able to constrain the non-linear variation component of the vertical motion that is predicted with distance to the trench.

The far field uplift rates for the central North Island predicted by the Savage model are lower than the observed rates (Fig. 7b). Indeed, in the central and eastern North Island (north of Cape Turnagain (Fig. 4 and inland) there is a broad uplift of about 1–3 mm/yr (Fig. 8). We ascribe this uplift to two general, long-term processes: sediment underplating above the subduction thrust as numerically outlined by Walcott (1987); and positive buoyancy in the mantle wedge due to the addition of melts generated in the mantle wedge (Fig. 8). Our preference for choosing a long term process is because geological evidence suggest uplift and exhumation of the central North Island has been ongoing since 5 Ma (Pulford and Stern, 2004). Seismic exploration show maximum sediment accumulations in excess of 5 km within the subduction channel beneath both ends of the Hikurangi Margin (Bassett et al., 2010; Henrys et al., 2013). These sediments accumulate down-dip on top of the subduction zone just above the Moho of the overriding plate (i.e. the Australian plate). "Underplating" of sediments on top of a quasi-rigid subducted lithosphere was first proposed to account for the lack of faulting linked to

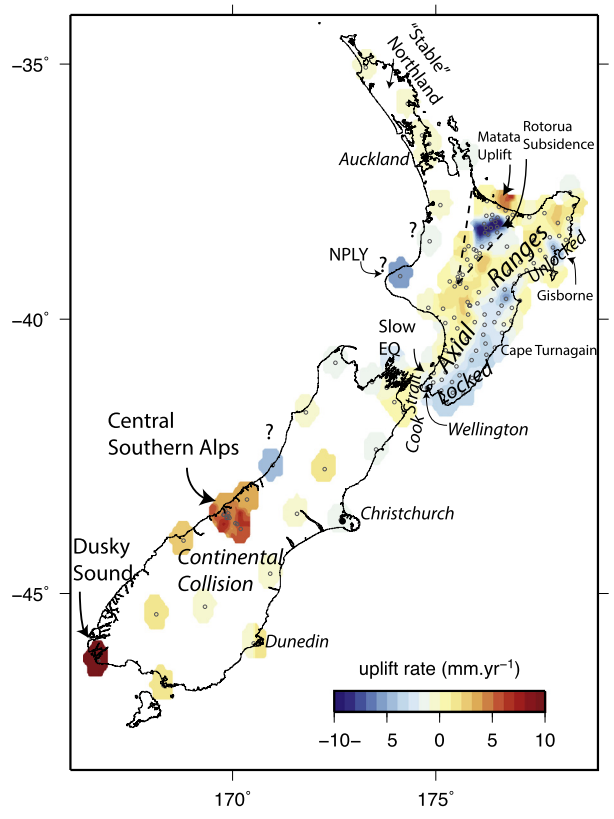

Fig. 4. Vertical velocities with annotated interpretations for regions of New Zealand. Open circles represent the locations of CGPS stations. Most values of uplift rates cluster to consistent regions apart from stations marked by question marks, as discussed in text. Stations for the central Southern Alps vertical GPS stations, which are not part of Geonet, are included (Beavan et al., 2010). Boundaries of the Central Volcanic Region are shown by the dashed lines (Molnar et al., 2015). Smoothing around sites have been completed using the function *nearneighbor* (Increment I = 10 km, Radius S = 30 km) of Generic Mapping Tools (Wessel et al., 2013).

the uplift of the axial ranges of the North Island (Walcott, 1987). Walcott (1987) makes reasonable assumptions about volume of sediment being subducted, degree of isostatic compensation, then suggests 2–3 mm/yr for uplift of the Axial Ranges due to underplating (Fig. 8).

3.4.3. Central North Island and the Volcanic Plateau

The wavelength of uplift signal for the central North Island is too wide (∼80 km) to be produced by underplating of the subduction zone by sediments, but does correlate well with recent volcanic activity in the area. Here we suggest the continental back-arc is being uplifted by positive buoyancy in the upper mantle (Fig. 8) provided by the intrusion of basaltic melts. Supporting evidence for mantle melts and positive buoyancy comes from rock uplift and seismic velocity studies (Pulford and Stern, 2004; Seward et al., 2009; Stern and Benson, 2011).

Colloquially, the central North Island is often referred to as "the Volcanic Plateau" (McKinnon, 2015) because of its active volcanism and broad elevation of around 300 m above sea level (Pulford and Stern, 2004). The boundaries of the Plateau are roughly coincident with those of the Central Volcanic Region (Fig. 4) as defined by Walcott (1987) and Stern (1987). Based on porosity of exhumed marine mudstones around the periphery of the Volcanic Plateau a rock uplift rate was calculated, with respect to mean sea-level, of 0.6 ± 0.1 mm/yr for the past 5 my (Pulford and Stern, 2004). Our decade-long cGPS data base suggest a 1–2 mm/yr uplift here, but the uncertainty is such that it may be that there is no significant difference between the two data sets. For the purpose of the model described below we adopt a rock uplift rate of 1 mm/yr.

Table 2
Values of variables adopted for use in Eq. (1).

Symbol	Parameter	Value for Central North Island
e	Surface elevation (+ve downwards)	−0.3 km
H_0	Elevation of buoyant asthenosphere	2.4 km
ρ_b	Density of basalt intrusion in mantle	2900 kg/m^3
ρ_a	Density of asthenosphere	3300 kg/m^3
ρ_s	Density of sediments	2200 kg/m^3
ρ_c	Density of crust	2800 kg/m^3
ε	Extensional strain rate (% per my)	20%
b	Rate of intrusion of basalt	Variable to solve for
s	Sedimentation or erosion rate	2 km/my
α	Coeff. of thermal expansion	3.5×10^{-5} °C^{-1}
c	Specific heat of rock	800 J/(kg °C)
Q	Heat flow	800 mW/m^2

Water from the subducted slab, causing melt in the mantle wedge (Stern, 2002), is one way of explaining a positive buoyancy and surface uplift in back-arc regions. If an area is under extension there will be competing vertical buoyancy stress due to both thinning of the crust, and mantle lithosphere, so that the net uplift rate (de/dt) is given by (Lachenbruch and Morgan, 1990):

$$\frac{de}{dt} = (H_0 - e)\varepsilon + \left(1 - \frac{\rho_b}{\rho_a}\right)b + \left(1 - \frac{\rho_s}{\rho_a}\right)s + \frac{\alpha}{\rho_c c}Q \qquad (1)$$

where: e is surface elevation; H_0 = is the elevation of sea level above the buoyant level of the asthenosphere; ε is the extensional strain rate of the crust; ρ is density with subscripts a, b, s representing asthenosphere, basalt intrusion and sediments respectively; b = rate of intrusion of basaltic sill into mantle asthenosphere; s = sedimentation or erosion rate; α = coefficient of thermal expansion; and c = specific heat. Values adopted in the calculation are shown in Table 2.

It is assumed the Central Volcanic Region is extending at a rate of 20% per million years i.e. $\sim 10^{-6}$/yr (Walcott, 1987) and it is ∼50 km wide. We then leave the b = thickness of intruded basalt into the asthenosphere and calculate what rate is needed to produce ∼1 mm/yr surface uplift. We find an intrusion rate of ∼6 mm/yr is required, or a 6 km thick layer in 1 my, or a cross-sectional volume of ∼300 km^3/km (of strike) in a million years. This is consistent with the heat output of $\sim 4.3 \times 10^9$ Watts, which if assumed to be steady state, requires, in a million years, a volume of molten rock of ∼240 km^3/km to solidify (Stern, 1987).

Although there are several approximations in Eq. (1), including a uniform density crust, the order of magnitude estimates for intrusion rate are plausible and suggest the uplift of the Volcanic Plateau can be explained by a process of low-density basaltic intrusion into the upper mantle. We do stress, however, that this model for uplift of the Volcanic Plateau is assuming the rate we observe on a decade of the cGPS data is a snapshot of the long term (i.e. million years) scale process. It is possible that the signal is just a short term phenomenon and that another model is required to explain it.

3.4.4. Elliptical-shaped subsidence along the central Taupo volcanic zone

In the middle of the Central Volcanic Region there is a distinct area of subsidence of $\sim 50 \times 50$ km across where horizontal extension is documented by up to 9 stations (Fig. 5a). The maximum rate of subsidence is about −14 mm/yr and has been previously studied with InSAR and GPS (Hamling et al., 2015). From the cGPS there is also evidence of uplift around the northern edges at stations RGMT and RGAR (Fig. 5a). Moreover, the time series in the Rotorua – Matata region (Fig. 6) show that the uplift and subsidence are coeval even though the RGMT site stops its rise almost 6 months before the subsiding sites (RGUT, RGHL, RGMK) halt their declines. This link in timing is a key constraint in assessing if the

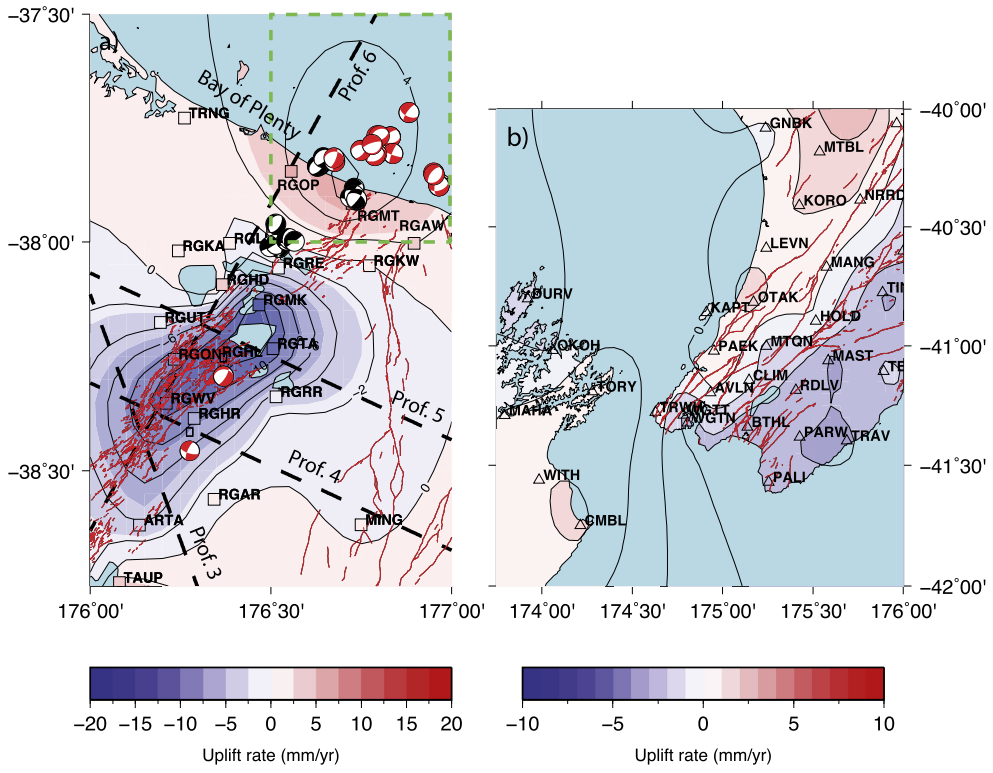

Fig. 5. Vertical surface motions in the areas of Rotorua (a) and Wellington (b). Subsidence is visible extending north–east of the Lake Taupo station (TAUP) along the Taupo Volcanic Zone (maximum amplitude of 14 mm/yr) while uplift of up to 3 mm/yr is seen along the Bay of Plenty coast line (between stations TRNG and RGAW). Subsidence along the east coast line of the North Island is ∼3 mm/yr. The seismicity that occurred during the 2008–2011 seismic swarm (Fig. A3) is shown in red. The seismicity that preceded the year 2008 is shown in black. The green dashed-line rectangle delimits the areas of the 2008–2011 Matata earthquake swarm as discussed in text used to plot Fig. A3. Profiles shown by black dashed lines are displayed in Fig. 7a. (For interpretation of the references to color in this figure legend, the reader is referred to the web version of this article.)

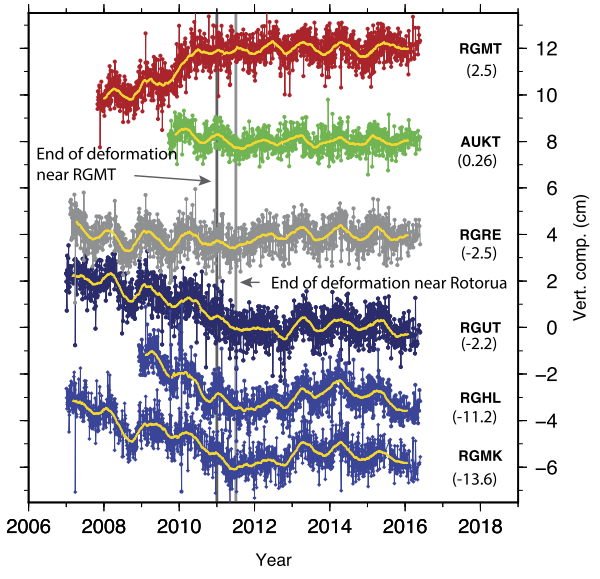

Fig. 6. Time series of vertical components for GPS stations located near and north of the Rotorua subsidence and in the area of Auckland with respect to Auckland (Figs. 3 and 4). We have detrended the time-series using the years 2012–2015 to make the change of displacement rate more visible. RGUT is on the flank of the subsiding region where we estimate the maximum subsidence rate is ∼4 mm/yr (Fig. 5.a). The other station is along the coast near Matata (RGMT) where there appears a coeval uplift of about 5 mm/yr. Note that both uplift and subsidence are coeval at RGUT, RGHL and RGMK) then terminate at mid-2011 (right line). At the site RGMT the deformation potentially ended 6 (left vertical line) to 8 months earlier. Monthly residuals vertical velocities are shown using orange curves. Horizontal motions of the same sub-network are shown in Fig. A2. (For interpretation of the references to color in this figure legend, the reader is referred to the web version of this article.)

uplift and subsidence seen here is magmatic (Hamling et al., 2016; Houlié et al., 2006b; Houlié and Montagner, 2007; Nishimura et al., 2001) or possibly tectonic (Scott and Stevenson, 1989), in origin.

Earthquake swarms around the settlement of Matata on the Bay of Plenty coast (Fig. 4) are common and have been documented since 1976 (Hurst et al., 2008; Rastin et al., 2013; Richardson, 1989). An association between these earthquake swarms and the area of uplift has been made (Hamling et al., 2016). The cGPS time series (Fig. 6) show that vertical movements in the Rotorua–Matata region (both uplift and subsidence) terminated abruptly at the beginning of 2012, as did the earthquake swarms (Fig. A3).

The width of the subsidence across the Rotorua anomaly (Fig. 5) is about 35 km, and the "half width" ($X_{0.5}$ = half the anomaly width at half the maximum value (Kearey and Brooks, 1991)) is ∼10 km. If we adopt a Mogi source (Mogi, 1958) to model the surface deformation, the maximum depth for the source is ∼1.3 $X_{0.5}$ (∼1 km). If we adopt a horizontal cylindrical source, given the elliptical character of the anomaly shape, the depth to its center would be about 10 km. These depths roughly correspond to the top of the underplated mafic rift ($V_p = 6.8$–7.1 km/s) pillow of Stern and Benson (2011) based on wide-angle seismic reflection and seismic refraction. Thus from a structural point of view there appears an association between mafic intrusion beneath the Central Volcanic Region and the development of either rhyolitic or basaltic magma movements immediately above the rift pillow.

Focal mechanisms of the 2008 Matata swarm (Rastin et al., 2013) and the 1977 swarm (Richardson, 1989) shows normal and strike-slip faulting north of the region of uplift (Fig. 5), and maximum focal depths ∼10 km. The area of subsidence, to the southwest, however, remained largely aseismic (Fig. 5). It is unclear what the causative relationship is between the areas of subsidence and uplift, particularly as their relative movements are well cor-

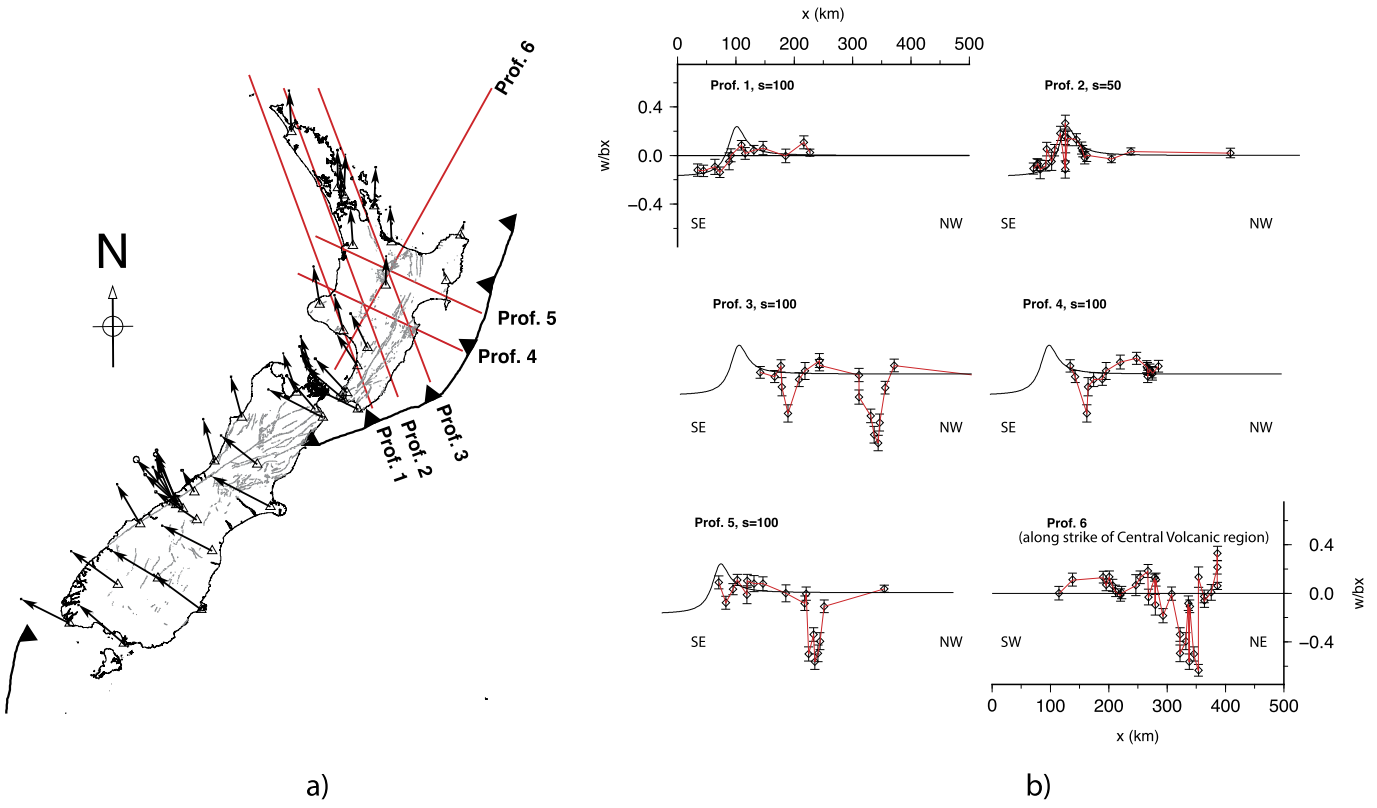

Fig. 7. a: Profiles used to model the interseismic uplift rates shown in Fig. 7.b. b: Vertical motions along 6 profiles across the North Island are shown against normalized uplift rates (w/bx) based on the elastic dislocation model of Savage (1983). Solid lines are calculated from the Savage model and red lines with open circles are observed data. w is the vertical displacement and b_x is the dip-slip component of slip on the subduction interface. Here we assume a dip angle for the subduction of 10° and a convergence rate 22 mm/yr, corresponding to half of the relative motion between New Zealand and Pacific plate. A value w/b_x of 0.4 corresponds to 8.8 mm/yr of vertical motion. For all profiles but profile 2, data are well explained by a value of downdip width of the main thrust zone $s = 100$ km. For profile 2, we adopt $s = 50$ km to accommodate locations where SSEs are observed. This suggests the lower part of the subduction is unloaded by large SSEs such as the Manawatu event (McCaffrey et al., 2008). (For interpretation of the references to color in this figure legend, the reader is referred to the web version of this article.)

related in time (Fig. 6). However, recent work ascribes the Matata uplift as being due to the intrusion of new magma (Hamling et al., 2016) and the subsidence in the Rotorua area as being due to contraction of cooling magma with an annual volume change of 0.011–0.016 km^3 (Hamling et al., 2015). A subsidence anomaly on a decade time and space scale similar to the one described here was also detected around the north shore of Lake Taupo from lake leveling data (Smith et al., 2007). They model a number of candidate processes but conclude that in order to explain the rapid time scale, and wavelength, of this anomaly a catastrophic process like sudden degassing or dewatering of rhyolitic magma is more likely than magma movement.

Vertical movements we see in the Rotorua area are also of a similar length and time scale to that reported in other volcanic-rift zones of the Earth such as Iceland (Hjartardóttir et al., 2012; Wright et al., 2012), East Africa (Biggs et al., 2009; Wright et al., 2012), Mt. Etna (Houlié et al., 2006a; Massonnet et al., 1995) and in the Andes (Henderson and Pritchard, 2013). A more detailed analysis of this intriguing transient motion, both subsidence and uplift, after careful integration of GPS data and estimation of the troposphere contribution (Houlié et al., 2016), is required but is beyond the scope of this paper.

3.4.5. Wellington region

West of Wellington and on both sides of Cook Strait (Fig. 4) there is a localized area of uplift of ∼1–2 mm/yr. This area, (i.e. labeled "slow EQ" on Fig. 4) has been subjected to slow earthquakes since at least 2003 (Wallace and Beavan, 2010), which appear to occur every 5 yr. Examination of the times series from TORY, PAEK, KAPT and OTAK show that the motion is down between slow slip events and up during the slow slip event (Wallace and Beavan, 2010). Averaged over 3 such cycles (PAEK, Fig. 2) the net effect is a small uplift. So even though the Kapiti coast area (north of Wellington city) is uplifting (1–2 mm/yr) at the about the same rate as sea level for New Zealand (Hannah, 2004) it is not clear if this net uplift would be sustained over many slow-slip event cycles. More data are needed to clarify the long-term motion for this region.

4. Conclusions

The intent of this study is to assess the quality of the vertical GPS velocity field after a decade of GPS deployment within a plate boundary, while attempting to isolate regional trends of either subsidence or uplift. A first attempt at making a vertical uplift rate map from cGPS in New Zealand was made from data collected by just 27 stations of the LINZ array over 8 yr (Houlié and Stern, 2012). At that time data points were too sparse to map local anomaly patterns with accuracy. In this study, the vertical rates of the 157 stations spanning up to 12 yr allow the detection of a more diverse, and accurate patterns of uplift. We show that the vertical cGPS field is consistent with our knowledge of geological vertical movements, on both short and log term time scales, and with regional tectonics. The absolute level of vertical movement may still have >2mm/yr uncertainty, due to base line issues, but the uncertainty on relative movement for different parts of the country are now in the 1–2 mm/yr range. This pattern will consolidate and improve with another ∼10 yr of data.

Key findings from the first decade of vertical cGPS in New Zealand are:

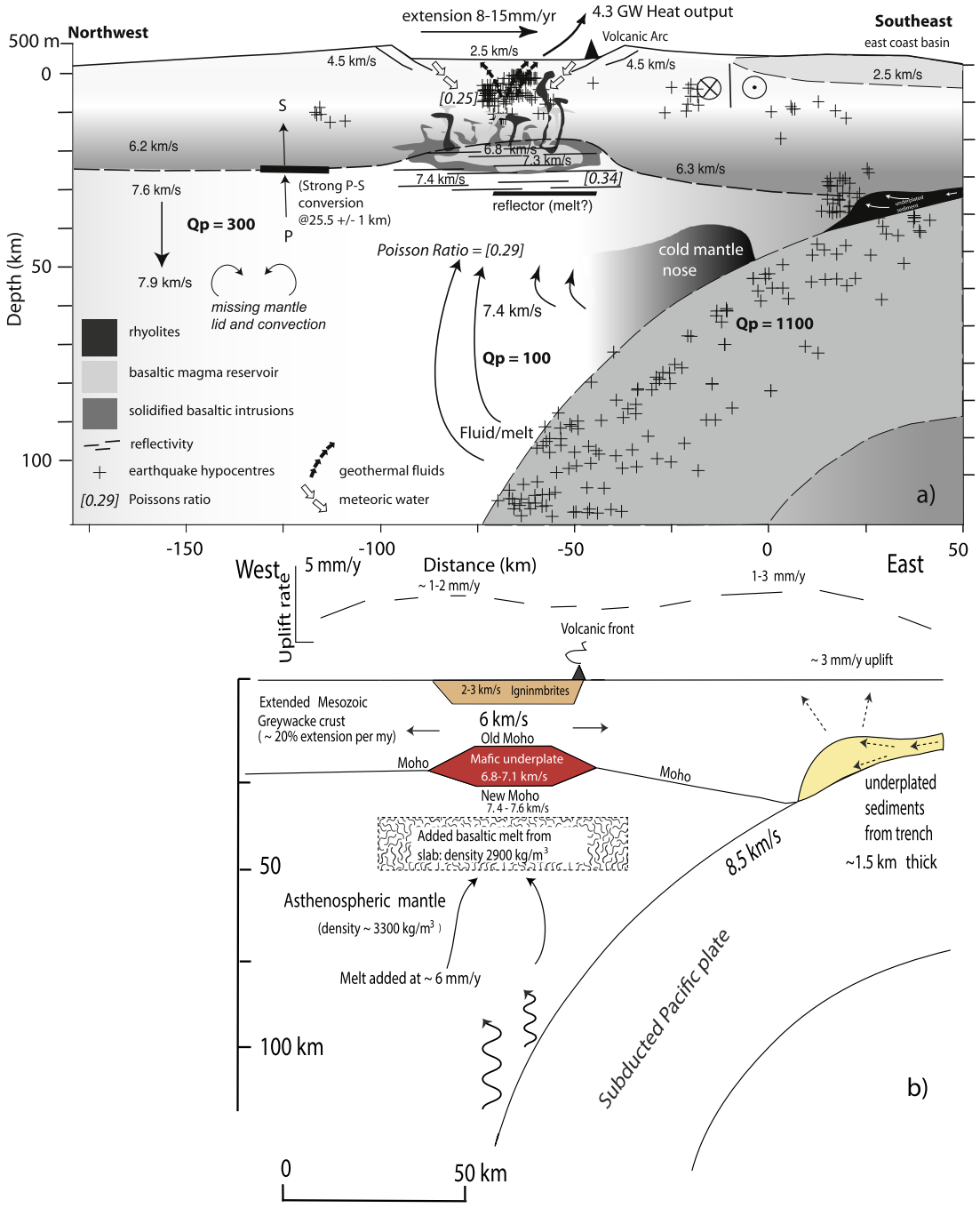

Fig. 8. a) Cross section through the central North Island based on active and passive source seismic studies showing crustal structure, seismic velocities, Poisson's ratio and Q. After Stern et al. (2010). b) A simplified parameterization of the crustal structure for the input to the Lachenbruch model (Lachenbruch and Morgan, 1990) as described in the text.

i. Relative to a fixed Northland–Auckland region much of New Zealand is undergoing a mild uplift (<0.5 mm/yr).
ii. Along the subduction margin of the eastern North Island are two distinct areas of subsidence and uplift, linked to locked (south) and unlocked (north) regions, respectively.
iii. Central North Island is characterized by a broad uplift that we interpret as due to both buoyancy from injected melts into the asthenospheric mantle, and underplating by sediments on the subduction zone.
iv. Within central North Island is the Rotorua anomaly, which is ~50 km by 50 km region of intense subsidence (up to −14 mm/yr). This appears to be related to active normal faulting, volcanism and earthquake swarms. We interpret this anomaly as being due to interplay between extension, degassing and possibly intrusion of magmas into the lower crust.
v. Around and just to north of Wellington the vertical GPS is dominated by slow slip events. Between slow slip events the subsidence is recorded that is then reversed by the slow slip event. Up to 3 cycles have been observed, each 5 yr apart. Some stations show net uplift and some subsidence depending on how long the record is and when it started.
vi. In the next 5–10 yr this data set will improve and the uncertainties will potentially decrease by a factor of two. When this happens it is likely that the vertical velocity field could become an important tool to seek precursor signals to earthquakes or slow slip.

Acknowledgements

We thank E. Smith and G. A. Houseman for reviews of earlier versions of this manuscript. This project was supported by ETH. Figs. 1–6 and A1–A3 have been drawn using Generic Mapping Tools (Wessel et al., 2013) and Adobe Illustrator CS6. Authors thank two anonymous reviewers who helped improving the initial manuscript. This work could not have been possible without the support of the ARC1/ARC2 team of the University of Leeds, UK.

Appendix A. Supplementary material

Supplementary material related to this article can be found online at http://dx.doi.org/10.1016/j.epsl.2016.10.018.

References

Altamimi, Z., Métivier, L., Collilieux, X., 2012. ITRF2008 plate motion model. J. Geophys. Res. 117.

Amos, C.B., Audet, P., Hammond, W.C., Bürgmann, R., Johanson, I.A., Blewitt, G., 2014. Uplift and seismicity driven by groundwater depletion in central California. Nature 509, 483–486.

Bassett, D., Sutherland, R., Henrys, S., Stern, T., Scherwath, M., Benson, A., Toulmin, S., Henderson, M., 2010. Three-dimensional velocity structure of the northern Hikurangi margin, Raukumara, New Zealand: implications for the growth of continental crust by subduction erosion and tectonic underplating. Geochem. Geophys. Geosyst. 11.

Beavan, J., Denys, P., Denham, M., Hager, B., Herring, T., Molnar, P., 2010. Distribution of present-day vertical deformation across the Southern Alps, New Zealand, from 10 years of GPS data. Geophys. Res. Lett. 37.

Beavan, J., Litchfield, N.J., 2012. Vertical Land Movement Around the New Zealand Coastline: Implications for Sea-Level Rise. GNS Sci. Report, 42 p.

Beavan, J., Matheson, D., Denys, P., Denham, M., Herring, T., Hager, B., Molnar, P., 2004. A vertical deformation profile across the Southern Alps, New Zealand, from 3.5 years of continuous GPS data. In: van Dam, T. (Ed.), The State of GPS Vertical Positioning Precision: Separation of Earth Processes by Space Geodesy. Cahiers de Centre Europeen de Geodynamique et Seismologie.

Bergeot, N., Bouin, M.N., Diament, M., Pelletier, B., Régnier, M., Calmant, S., Ballu, V., 2009. Horizontal and vertical interseismic velocity fields in the Vanuatu subduction zone from GPS measurements: evidence for a central Vanuatu locked zone. J. Geophys. Res. 114.

Biggs, J., Anthony, E.Y., Ebinger, C.J., 2009. Multiple inflation and deflation events at Kenyan volcanoes, East African Rift. Geology 37, 979–982.

Bradley, S.L., Milne, G.A., Teferle, F.N., Bingley, R.M., Orliac, E.J., 2009. Glacial isostatic adjustment of the British Isles: new constraints from GPS measurements of crustal motion. Geophys. J. Int. 178, 14–22.

Ching, K.-E., Hsieh, M.-L., Johnson, K.M., Chen, K.-H., Rau, R.-J., Yang, M., 2011. Modern vertical deformation rates and mountain building in Taiwan from precise leveling and continuous GPS observations, 2000–2008. J. Geophys. Res. 116.

Cox, S.C., Stirling, M.W., Herman, F., Gerstenberger, M., Ristau, J., 2012. Potentially active faults in the rapidly eroding landscape adjacent to the Alpine Fault, central Southern Alps, New Zealand. Tectonics 31, n/a–n/a.

Delahaye, E.J., Townend, J., Reyners, M.E., Rogers, G., 2009. Microseismicity but no tremor accompanying slow slip in the Hikurangi subduction zone, New Zealand. Earth Planet. Sci. Lett. 277, 21–28.

Dimitrova, L.L., Wallace, L.M., Haines, A.J., Williams, C.A., 2016. High-resolution view of active tectonic deformation along the Hikurangi subduction margin and the Taupo Volcanic Zone, New Zealand. N.Z. J. Geol. Geophys. 59, 43–57.

Eiby, G., 1958. The structure of New Zealand from seismic evidence. Geol. Rundsch. 47, 647–662.

GNS New Zealand, 2015. New Zealand active faults database 250 K.

Gurnis, M., Müller, R.D., Moresi, L., 1998. Cretaceous vertical motion of Australia and the Australian–Antarctic discordance. Science 279, 1499–1504.

Hamling, I.J., Hreinsdóttir, S., Bannister, S., Palmer, N., 2016. Off-axis magmatism along a subaerial back-arc rift: observations from the Taupo Volcanic Zone, New Zealand. Sci. Adv. 2.

Hamling, I.J., Hreinsdóttir, S., Fournier, N., 2015. The ups and downs of the TVZ: geodetic observations of deformation around the Taupo Volcanic Zone, New Zealand. J. Geophys. Res., Solid Earth 120, 4667–4679.

Hammond, W.C., Blewitt, G., Li Zhenhong, Z., Plag, H.-P., Kreemer, C., 2012. Contemporary uplift of the Sierra Nevada, western United States, from GPS and InSAR measurements. Geology, vol. 40, pp. 667–670.

Hannah, J., 2004. An updated analysis of long-term sea level change in New Zealand. Geophys. Res. Lett. 31.

Henderson, S.T., Pritchard, M.E., 2013. Decadal volcanic deformation in the Central Andes Volcanic Zone revealed by InSAR time series. Geochem. Geophys. Geosyst. 14, 1358–1374.

Henrys, S., Wech, A., Sutherland, R., Stern, T., Savage, M., Sato, H., Mochizuki, K., Iwasaki, T., Okaya, D., Seward, A., Tozer, B., Townend, J., Kurashimo, E., Iidaka, T., Ishiyama, T., 2013. SAHKE geophysical transect reveals crustal and subduction zone structure at the southern Hikurangi margin, New Zealand. Geochem. Geophys. Geosyst. 14, 2063–2083.

Herman, F., Rhodes, E.J., Braun, J., Heiniger, L., 2010. Uniform erosion rates and relief amplitude during glacial cycles in the Southern Alps of New Zealand, as revealed from OSL-thermochronology. Earth Planet. Sci. Lett. 297, 183–189.

Herring, T.A., 2003. GLOBK: Global Kalman Filter VLBI and GPS Analysis Program Version 10.1. Massachusetts Institute of Technology, Cambridge.

Hjartardóttir, A.R., Einarsson, P., Bramham, E., Wright, T.J., 2012. The Krafla fissure swarm, Iceland, and its formation by rifting events. Bull. Volcanol. 74, 2139–2153.

Houlié, N., Montagner, J.-P., 2007. Hidden Dykes detected on Ultra Long Period seismic signals at Piton de la Fournaise volcano? Earth Planet. Sci. Lett. 261, 1–8.

Houlié, N., Briole, P., Bonforte, A., Puglisi, G., 2006a. Large scale ground deformation of Etna observed by GPS between 1994 and 2001. Geophys. Res. Lett. 33.

Houlié, N., Komorowski, J.C., de Michele, M., Kasereka, M., Ciraba, H., 2006b. Early detection of eruptive dykes revealed by normalized difference vegetation index (NDVI) on Mt. Etna and Mt. Nyiragongo. Earth Planet. Sci. Lett. 246, 231–240.

Houlié, N., Funning, G., Bürgmann, R., 2016. Use of a GPS-derived troposphere model to improve InSAR deformation estimates in the San Gabriel Valley, California. IEEE Trans. Geosci. Remote Sens. 54, 5365–5374.

Houlié, N., Stern, T., 2012. A comparison of GPS solutions for strain and SKS fast directions: implications for modes of shear in the mantle of a plate boundary zone. Earth Planet. Sci. Lett. 345–348, 117–125.

Houlié, N., Woessner, J., Giardini, D., Rothacher, M., submitted for publication. Lithosphere strain rate and stress field orientations across the Alpine front. Nat. Commun.

Howell, S., Smith-Konter, B., Frazer, N., Tong, X., Sandwell, D., 2016. The vertical fingerprint of earthquake cycle loading in southern California. Nat. Geosci.

Hurst, T., Bannister, S., Robinson, R., Scott, B., 2008. Characteristics of three recent earthquake sequences in the Taupo Volcanic Zone, New Zealand. Tectonophysics 452, 17–28.

Issac, M.J., 1996. Geology of Kaitaia Area. Institute of Geological and Nuclear Sciences, p. 1:250 000 Geological Map.

Kaneko, Y., Avouac, J.-P., Lapusta, N., 2010. Towards inferring earthquake patterns from geodetic observations of interseismic coupling. Nat. Geosci. 3, 363–369.

Kearey, P., Brooks, M., 1991. An Introduction to Geophysical Exploration, 2nd edition. Blackwell Scientific Publications, Oxford.

King, R., Bock, Y., 2012. GAMIT User Manual.

Koons, P.O., 1990. Two-sided orogen: collision and erosion from the sandbox to the Southern Alps, New Zealand. Geology 18, 679–682.

Lachenbruch, A.H., Morgan, P., 1990. Continental extension, magmatism, and elevation; formal relations and rules of thumb. Tectonophysics 174, 39–62.

Lamb, S., Smith, E., 2013. The nature of the plate interface and driving force of interseismic deformation in the New Zealand plate-boundary zone, revealed by the continuous GPS velocity field. J. Geophys. Res. 118, 2169–9356.

Lamb, S.H., Smith, E., Stern, T., Warren-Smith, E., 2015. Continent-scale strike-slip on a low-angle fault beneath New Zealand's Southern Alps: implications for crustal thickening in oblique collision zones. Geochem. Geophys. Geosyst. 16, 3076–3096.

Liang, S., Gan, W., Shen, C., Xiao, G., Liu, J., Chen, W., Ding, X., Zhou, D., 2013. Three-dimensional velocity field of present-day crustal motion of the Tibetan Plateau derived from GPS measurements. J. Geophys. Res., Solid Earth 118, 5722–5732.

Massonnet, D., Briole, P., Arnaud, A., 1995. Deflation of Mount Etna monitored by spaceborne radar interferometry. Nature 375, 567–570.

McCaffrey, R., Wallace, L.M., Beavan, J., 2008. Slow slip and frictional transition at low temperature at the Hikurangi subduction zone. Nat. Geosci. 1, 316–320.

McKinnon, M., 2015. Volcanic Plateau region. In: Te Ara – the Encyclopedia of New Zealand, pp. 1–16. http://www.teara.govt.nz/en/volcanic-plateau-region.

Mogi, K., 1958. Relations between the eruptions of various volcanoes and the deformations of the ground surfaces around them. Bull. Earthq. Res. Inst. Univ. Tokyo 36, 99–134.

Molnar, P., 2015. Gravitational instability of mantle lithosphere and core complexes. Tectonics 34, 478–487.

Molnar, P., England, P.C., Jones, C.H., 2015. Mantle dynamics, isostasy, and the support of high terrain. J. Geophys. Res., Solid Earth 120, 1932–1957.

Nibourel, L., Herman, F., Cox, S.C., Beyssac, O., Lavé, J., 2015. Provenance analysis using Raman Spectroscopy of Carbonaceous Material: a case study in the Southern Alps of New Zealand. J. Geophys. Res., Earth Surf. 120.

Nishimura, T., Shinzaburo, O., Murakami, M., Sagiya, T., Tada, T., Kaidzu, M., Ukawa, M., 2001. Crustal deformation caused by magma migration in the northern Izu Islands, Japan. Geophys. Res. Lett. 28, 3745–3748.

Ota, Y., Pillans, B., Berryman, K., Beu, A., Fujimori, T., Miyauchi, T., Berger, G., Beu, A.G., Climo, F.M., 1996. Pleistocene coastal terraces of Kaikoura Peninsula and the Marlborough coast, South Island, New Zealand. N.Z. J. Geol. Geophys. 39, 51–73.

Pillans, B., 1986. A Late Quaternary uplift map for North Island, New Zealand. Bull. R. Soc. N. Z. 24, 409–417.

Pillans, B., 1990. Pleistocene marine terraces in New Zealand: a review. N.Z. J. Geol. Geophys. 33, 219–231.
Pulford, A., Stern, T., 2004. Pliocene exhumation and landscape evolution of central North Island, New Zealand: the role of the upper mantle. J. Geophys. Res. 109.
Rastin, S.J., Unsworth, C.P., Benites, R., Gledhill, K.R., 2013. Using real and synthetic waveforms of the Matata swarm to assess the performance of New Zealand GeoNet phase pickers. Bull. Seismol. Soc. Am. 103, 2173–2187.
Reyners, M., 1989. New Zealand seismicity 1964–87: an interpretation. N.Z. J. Geol. Geophys. 32, 307–315.
Richardson, W.P., 1989. The Matata earthquake of 1977 May 31: a recent event near Edgecumbe, Bay of Plenty, New Zealand. N.Z. J. Geol. Geophys. 32, 17–30.
Savage, J.C., 1983. A dislocation model of strain accumulation and release at a subduction zone. J. Geophys. Res. 88, 4984–4996.
Scherwath, M., Stern, T.A., Davey, F.J., Okaya, D., Holbrooke, W.S., Davies, R., Kleffmann, S., 2003. Lithospheric structure across oblique continental collision in New Zealand from wide-angle P-wave modeling. J. Geophys. Res.
Scott, D.R., Stevenson, D.J., 1989. A self-consistent model of melting, magma migration, and buoyancy-driven circulation beneath mid-ocean ridges. J. Geophys. Res. 94, 2973–2988.
Sella, G.F., Stein, S., Dixon, T.H., Craymer, M., James, T.S., Mazzotti, S., Dokka, R.K., 2007. Observation of glacial isostatic adjustment in “stable” North America with GPS. Geophys. Res. Lett. 34.
Serpelloni, E., Faccenna, C., Spada, G., Dong, D., Williams, S.D.P., 2013. Vertical GPS ground motion rates in the Euro-Mediterranean region: new evidence of velocity gradients at different spatial scales along the Nubia–Eurasia plate boundary. J. Geophys. Res., Solid Earth 118, 6003–6024.
Seward, A.M., Henderson, C.M., Smith, E.G.C., 2009. Models of upper mantle beneath the Central North Island, New Zealand, from speeds and anisotropy of sub-horizontal P-waves (Pn). J. Geophys. Res. 114, B01301.
Smith, E.G.C., Wliliams, T.D., Darby, D.J., 2007. Principal component analysis and modelling of the subsidence of the shoreline of Lake Taupo, New Zealand, 1983–1999: evidence for dewatering of a magmatic intrusion? J. Geophys. Res. 112.
Steckler, M., 1985. Uplift and extension at the Gulf of Suez: indications of induced mantle convection. Nature 317, 135.
Stern, R.J., 2002. Subduction zones. Rev. Geophys. 40, 3-1–3-38.
Stern, T., Benson, A., 2011. Wide-angle seismic imaging beneath an andesitic arc: Central North Island, New Zealand. J. Geophys. Res., Solid Earth 116.
Stern, T., Stratford, W., Seward, A., Henderson, M., Savage, M., Smith, E., Benson, A., Greve, S., Salmon, M., 2010. Crust–mantle structure of the central North Island, New Zealand, based on seismological observations. J. Volcanol. Geotherm. Res. 190, 58–74.
Stern, T.A., 1987. Asymmetric back-arc spreading, heat-flux and structure associated with the central volcanic region of New-Zealand. Earth Planet. Sci. Lett. 85, 265–276.
Teferle, F.N., Bingley, R.M., Orliac, E.J., Williams, S.D.P., Woodworth, P.L., McLaughlin, D., Baker, T.F., Shennan, I., Milne, G.A., Bradley, S.L., Hansen, D.N., 2009. Crustal motions in Great Britain: evidence from continuous GPS, absolute gravity and Holocene sea level data. Geophys. J. Int. 178, 23–46.
Thatcher, W., 2003. GPS constraints on the kinematics of continental deformation. Int. Geol. Rev. 45, 191–212.
Tikoff, B., Teyssier, C., 1994. Strain modeling of displacement-field partitioning in transpressional orogens. J. Struct. Geol. 16, 1575–1588.
Walcott, D., 1984. The kinematics of the plate boundary zone through New Zealand: a comparison of short- and long-term deformations. Geophys. J. R. Astron. Soc. 79, 613–633.
Walcott, R.I., 1987. Geodetic strain and the deformation history of the North Island of New Zealand during the late Cenozoic. Philos. Trans. R. Soc. Lond. Ser. A, Math. Phys. Sci. 321, 163–181.
Wallace, L.M., Beavan, J., 2006. A large slow slip event on the central Hikurangi subduction interface beneath the Manawatu region, North Island, New Zealand. Geophys. Res. Lett. 33.
Wallace, L.M., Beavan, J., 2010. Diverse slow slip behavior at the Hikurangi subduction margin, New Zealand. J. Geophys. Res. 115.
Wdowinski, S., Bock, Y., Zhang, J., Fang, P., Genrich, J., 1997. Southern California Permanent GPS Geodetic Array: spatial filtering of daily positions for estimating coseismic and postseismic displacements induced by the 1992 Landers earthquake. J. Geophys. Res., Solid Earth 102, 18057–18070.
Wessel, P., Smith, W.H.F., Scharroo, R., Luis, J.F., Wobbe, F., 2013. Generic Mapping Tools: improved version released. Eos 94, 409–410.
Wright, T.J., Sigmundsson, F., Pagli, C., Belachew, M., Hamling, I.J., Brandsdóttir, B., Keir, D., Pedersen, R., Ayele, A., Ebinger, C., Einarsson, P., Lewi, E., Calais, E., 2012. Geophysical constraints on the dynamics of spreading centres from rifting episodes on land. Nat. Geosci. 5, 242–250.